Growth and division of active droplets provides a model for protocells

David Zwicker[1,2][†], Rabea Seyboldt[1][†], Christoph A. Weber[1], Anthony A. Hyman[3] and Frank Jülicher[1]★

It has been proposed that during the early steps in the origin of life, small droplets could have formed via the segregation of molecules from complex mixtures by phase separation. These droplets could have provided chemical reaction centres. However, whether these droplets could divide and propagate is unclear. Here we examine the behaviour of droplets in systems that are maintained away from thermodynamic equilibrium by an external supply of energy. In these systems, droplets grow by the addition of droplet material generated by chemical reactions. Surprisingly, we find that chemically driven droplet growth can lead to shape instabilities that trigger the division of droplets into two smaller daughters. Therefore, chemically active droplets can exhibit cycles of growth and division that resemble the proliferation of living cells. Dividing active droplets could serve as a model for prebiotic protocells, where chemical reactions in the droplet play the role of a prebiotic metabolism.

Living systems consist of cells that can grow and divide. Cells take up matter from the outside world to grow, they release waste products, and they are able to divide, creating more cells. A fundamental question is to understand how cells arose early in evolution. Early in the origin of life, chemical reaction centres or chemical microreactors had to form to organize chemical reactions in space. These microreactors had to exchange material with the outside and they had to propagate. Recently, the idea of Oparin and Haldane[1,2] that small droplets, which they called coacervates, could organize molecules in microreactors has resurfaced to prominence[3–8]. Such droplets are liquid-like aggregates that concentrate molecules that have separated from a complex mixture.

Liquid droplets are self-organized structures that coexist with a surrounding fluid[7,9]. The interface separating the two coexisting phases provides them with a well-defined surface. The associated surface tension forces them into a spherical shape. Furthermore, many substances can diffuse across the interface. The segregation of components into a droplet concentrates material in a confined volume, which may facilitate specific chemical reactions. Thus, droplets provide containers in which chemical reactions can be spatially organized. Although the thermodynamics of phase transitions can explain how liquid drops can form, it is unclear how such droplets could propagate by division and subsequent growth, an ability that would be key at the origin of life.

Droplets grow by taking up material from a supersaturated environment or by Ostwald ripening[9–13]. Ostwald ripening describes the exchange of material between droplets by diffusion, usually leading to growth of large droplets while small droplets shrink. Furthermore, droplets can increase in size by fusion of two droplets into a larger one. These processes lead to the formation of droplets of increasing size while the droplet number decreases with time. This behaviour is opposite to that of cells, which have a characteristic size and increase their number by division. How could droplets divide and propagate?

We have recently shown that droplets that are maintained away from thermodynamic equilibrium by a chemical fuel can have unusual properties[14,15]. In particular, in the presence of chemical reactions, Ostwald ripening can be suppressed[15] and multiple droplets can stably coexist, with a characteristic size set by the reaction rates[15–18]. Here, we show that, surprisingly, spherical droplets subject to chemical reactions spontaneously split in two smaller daughter droplets of equal size. Therefore, chemically active droplets can grow and subsequently divide and thereby propagate by using up the inflowing material as a fuel. We conclude that droplets can indeed behave similarly to cells in the presence of chemical reactions that are driven by an external fuel reservoir. Such active droplets could represent models for growing and dividing protocells with a rudimentary metabolism that is represented by simple chemical reactions that are maintained by an external fuel.

Division of active droplets

Droplets can serve as small compartments to spatially organize chemical reactions. The emergence of droplets requires phase separation into two coexisting liquid phases of different composition. Phase separation is driven by molecular interactions, where molecules with an affinity for each other lower their energy if they come closely together. A fluid can demix if the energy decrease associated with molecular interactions overcomes the effects of entropy increase by mixing[19,20]. If those interactions are strong, a sharp interface separates the coexisting phases.

Droplets can become chemically active if the material of the droplet is produced and destroyed by chemical reactions. An example that resembles a simple protocell is shown schematically in Fig. 1a. The droplet is formed by a droplet material D that is generated inside the droplet from a high-energy precursor N, which plays the role of a nutrient. Droplet material can degrade into a lower energy component W that plays the role of a waste, which leaves the droplet by diffusion. The droplet can survive if N is continuously supplied and W is continuously removed. This can be achieved by recycling N using an external energy source such as a fuel or radiation.

Inspired by Oparin[21], we discuss the physics of such active droplets using a simple model with only two components A and B (see Fig. 1b). The droplet material B phase separates from

---

[1]Max Planck Institute for the Physics of Complex Systems, 01187 Dresden, Germany. [2]School of Engineering and Applied Sciences, Harvard University, Cambridge, Massachusetts 02138, USA. [3]Max Planck Institute of Molecular Cell Biology and Genetics, 01307 Dresden, Germany. [†]These authors contributed equally to this work. *e-mail: julicher@pks.mpg.de
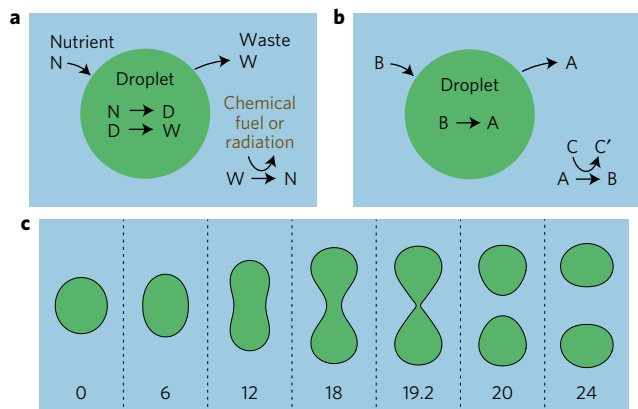
Figure 1 | Division of chemically active droplets. a, Schematic representation of an active droplet as a simple model of a protocell. The droplet (green) consists of a droplet material D. Nutrients N of high chemical energy can diffuse into the droplet. Inside the droplet, N is transformed to D by chemical reactions. Droplet material D is degraded chemically into low-energy waste W that leaves the droplet. **b**, Simple model, with droplet material B and soluble component A. The system is driven by a chemical fuel C that is transformed to the reaction product C′. **c**, Sequence of shapes of a dividing droplet at different times as indicated. The dynamic equations of a continuum model corresponding to the situation shown in **b** were solved numerically. The droplet shapes are shown as equal concentration contours (black). Parameter values are $\nu_- t_0/\Delta c = 7 \times 10^{-3}$, $\nu_+ t_0/\Delta c = 1.9 \times 10^{-3}$, and $k_\pm t_0 = 10^{-2}$, where t_0 is a characteristic time of the continuum model (see Supplementary Information). Indicated times are given in units of $10^2 t_0$.

the solvent. It can spontaneously be degraded by a chemical reaction

$$B \rightarrow A \qquad (1)$$

into molecules of type A that are soluble in the background fluid and leave the droplet. The backward reaction A → B is not proceeding spontaneously because B is of higher energy than A. New droplet material B can be produced by the second reaction

$$A + C \rightarrow B + C' \qquad (2)$$

that is coupled to a fuel C. Here C′ is the low-energy reaction product of the fuel molecules. The chemical potential difference $\Delta\mu_C = \mu_C - \mu_{C'} > 0$ provided by the fuel powers the production of high-energy B from low-energy A. The difference $\Delta\mu_C$ can be maintained constant if the concentrations of C and C′ are set by an external reservoir. In this case, the system is kept away from a thermodynamic equilibrium (see Fig. 2 and Methods).

The combination of phase separation and non-equilibrium chemical reactions can be studied in a continuum model[15–17] (see Supplementary Information). Using this model, we find that spherical droplets that are chemically active can undergo a shape instability and split into two smaller droplets, despite their surface tension (see Fig. 1c and Supplementary Movie). A droplet first grows until it reaches its stationary size[15]. Then, the droplet starts to elongate and forms a dumbbell shape. This dumbbell splits into two smaller droplets of equal size. The resulting smaller droplets grow again until a new division may occur, reminiscent of living cells.

To investigate the stability of spherical droplets, we study the droplet shape by an effective droplet model (see Fig. 3 and Methods). Figure 4a shows the behaviour of the stationary droplet radius in this model as a function of the supersaturation ϵ. This supersaturation is the excess concentration of droplet material far from the droplet,
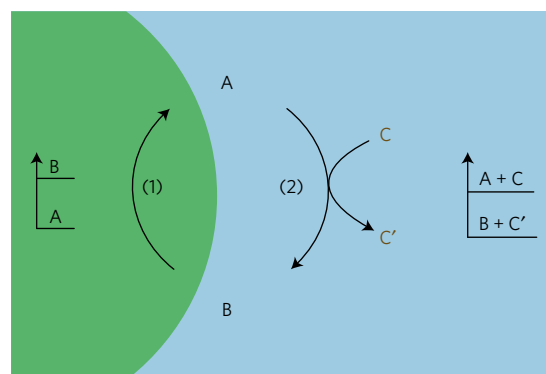

Figure 2 | Reaction rates and energy supply. Schematic representation of the reaction cycle involving the two pathways (1) and (2). The differences of the chemical potentials μ determine the direction of the spontaneous reactions: coupling to the chemical fuel C with reaction product C′ drives reaction pathway (2) in the direction A → B outside the droplet. Inside the droplet, where the concentration of C is smaller, reaction pathway (1) in the direction B → A dominates. See Methods and the Supplementary Information for details.

generated by the chemical reaction (2). For $\epsilon > 0$, material diffuses to the droplet and is incorporated. Figure 4a shows that for a given turnover ν_- of droplet material inside the droplet (see Methods), stationary droplets exist only for sufficiently large supersaturation. Beyond this threshold, droplets smaller than the critical radius (Fig. 4a, black dotted lines) shrink, while larger droplets grow toward the stationary radius (Fig. 4a, black solid line)[15]. At this stationary radius, the influx of B due to the supersaturation outside is balanced by the efflux of material A produced inside the droplet. Thus, a larger turnover leads to smaller droplets (Fig. 4a).

Droplet division occurs when a spherical droplet becomes unstable and elongates. We performed a linear stability analysis of spherical droplets at their stationary radius in the effective droplet model (see Supplementary Methods). We find that for increasing supersaturation ϵ, a spherical droplet with surface tension undergoes a shape instability when its radius reaches a critical value R_{div} that depends on the reaction rates and droplet parameters (see Fig. 4a). Beyond the radius R_{div}, the spherical shape is unstable and any small shape deformation triggers the elongation of the droplet shape along one axis.

The stability analysis of the effective droplet model can be represented in a state diagram (see Fig. 4b). We find three different regions as a function of supersaturation ϵ and turnover of droplet material ν_-. A region where droplets do not exist (white), a region in which spherical droplets are stable (blue), and a region in which spherical droplets are unstable (red).

To study how the shape instability leads to droplet division, we investigated the droplet dynamics beyond the linearized analysis using the continuum model. This model can capture the topological changes of the droplet surface that occur during division. Numerical calculations of the continuum model (see Supplementary Information) confirm the results of the stability analysis. An example of droplet division is shown in Fig. 1c. The state diagram for the continuum model is shown in Fig. 4c. Comparing the state diagrams Fig. 4b and Fig. 4c reveals that both models exhibit qualitatively the same behaviours. Note that due to simplifications in the effective droplet model, the parameters are different in both models (see Supplementary Information) and the regions in both diagrams differ slightly. While Fig. 4b shows only where droplets become unstable (red line), Fig. 4c reveals the behaviours of droplets in the unstable region. We find that droplets typically divide into two daughters (red circles). However, for some
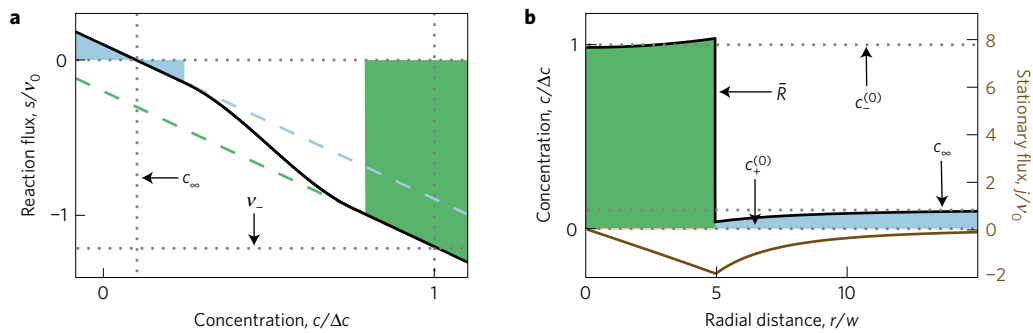
Figure 3 | Reaction flux, concentration profile and diffusion flux in an effective droplet model. Shaded regions correspond to concentration ranges inside (green) and outside the droplet (blue). **a**, Chemical reaction flux s as a function of concentration (black). The linearized fluxes inside (green) and outside the droplet (blue) are indicated as dashed lines. **b**, Stationary concentration profile of the droplet material B (black) and stationary flux $j = -D_\pm \partial_r c$ (brown, axis on the right). The droplet radius $\bar{R}$, the equilibrium concentrations $c_\pm^{(0)}$, and the concentration far from the droplet c_∞ are indicated. The corresponding supersaturation is defined as $\epsilon = (c_\infty - c_+^{(0)})/\Delta c$ (see Methods). Parameter values are: $k_\pm \tau_0 = 10^{-2}$, $c_+^{(0)} = 0$, $\beta_- = \beta_+$, $D_- = D_+$, $v_0 = 10^{-2} \Delta c / \tau_0$, $v_-/v_0 = 1.2$ and $v_+/v_0 = 0.1$.
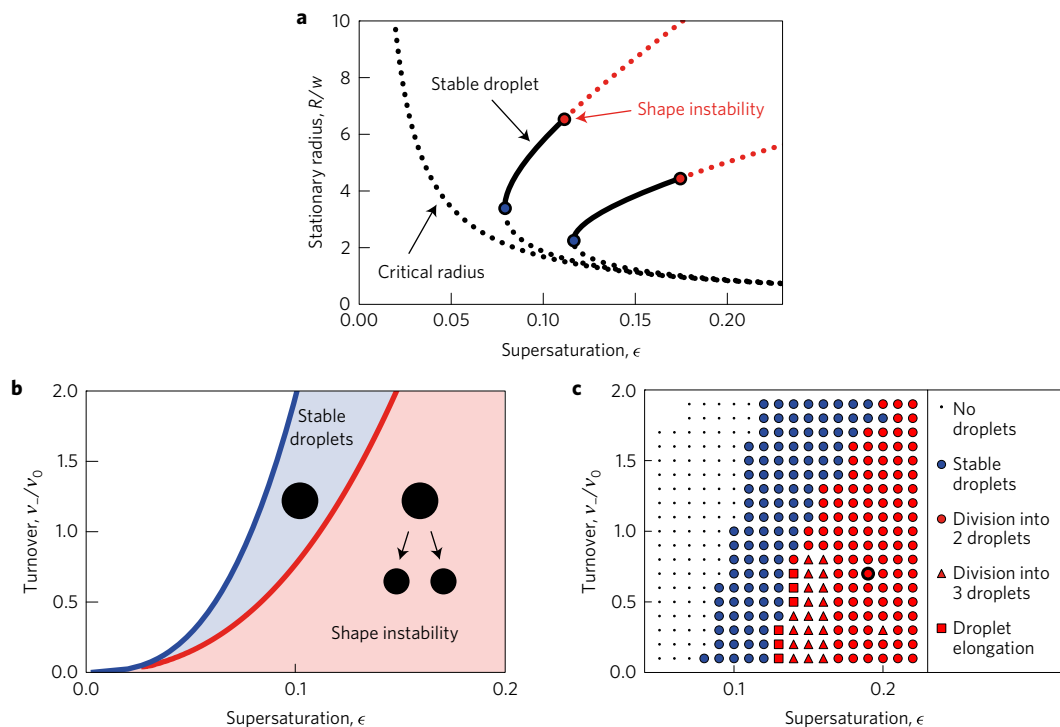

Figure 4 | Stationary droplet radii and stability diagrams. a, Stationary radii of active droplets. The droplet radius R of spherical droplets is shown as a function of supersaturation ϵ for different values of normalized turnover $v_-/v_0 = 0, 1, 3$ (from left to right). Radii of stable droplets are shown as solid black lines. Dotted lines indicate states where droplets are unstable with respect to size (black) or shape (red). The results are obtained for the effective droplet model described in the Methods. Parameter values are: $k_\pm \tau_0 = 10^{-2}$, $c_+^{(0)} = 0$, $\beta_- = \beta_+$, $D_- = D_+$ and $v_0 = 10^{-2} \Delta c / \tau_0$. Here, $w = 6\beta_+ \gamma / \Delta c$, and $\tau_0 = w^2/D_+$ are characteristic length and time scales. **b**, Stability diagram of active droplets as a function of supersaturation $\epsilon = v_+/(k_+ \Delta c)$ and turnover v_- of droplet material. Droplets either dissolve and disappear (white region), are spherical and stable (blue region), or undergo a shape instability and typically divide (red region). The lines of instability are obtained for the droplet model described in the Methods for the same parameters as in **a**. **c**, The same stability diagram as in **b** but for the continuum model described in the Supplementary Information. The behaviour of droplets is indicated by symbols for different values of v_- and ϵ. Parameter values are $k_\pm t_0 = 10^{-2}$ (see Supplementary Information). The parameter values corresponding to Fig. 1c are indicated (large red circle).

parameter values they divide into three droplets (red triangles). In a few cases, division was not seen during the time of calculations (red squares). In these cases droplets elongated until they reached the size of the simulation box. It is unclear whether they would divide in a larger box.

Our numerical calculations also reveal that droplets typically undergo multiple divisions (see Fig. 5a and Supplementary Movie). After a first division, the smaller daughters grow until they divide again when they reach the radius R_{div}. Interestingly, the

division axes are not independent of each other (see Fig. 5a). In the absence of system boundaries, the division axes of both daughters are perpendicular to the first division axis (see Fig. 5b). Similarly, when the four granddaughters divide, their division axes are perpendicular to both the division axes of the first and the second division. The division axes in subsequent droplet divisions are determined by droplet interactions via the concentration fields surrounding the droplets. The two growing daughter droplets effectively compete for droplet material, leading
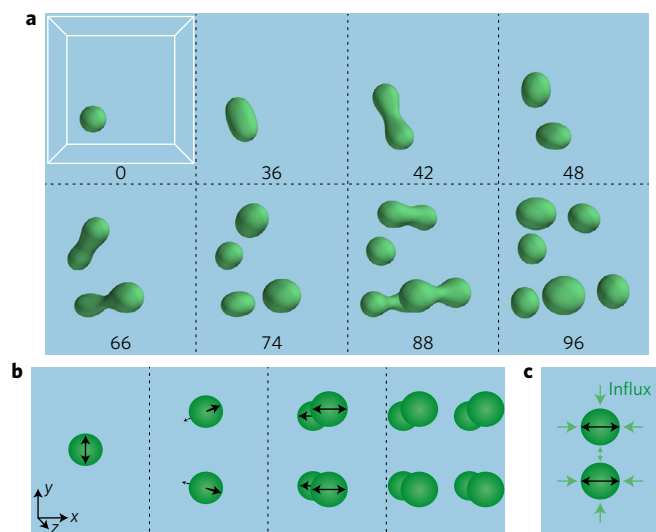
Figure 5 | Cycles of growth and divisions. a, Sequence of droplet divisions at different times as indicated in units of $10^2 t_0$. Droplet configurations obtained from numerical solutions to the continuum model are represented as three-dimensional shapes. Parameter $\nu_+ t_0/\Delta c = 2 \times 10^{-3}$. Remaining parameters are the same as in Fig. 1c. **b**, Schematic representation of the orientation of subsequent division axes. **c**, Droplet division is oriented along the axis for which diffusion fluxes (green arrows) are maximal.

to the depletion of droplet material in the space between them. Therefore, diffusion fluxes and growth rates are larger along axes perpendicular to the previous division axis (see Fig. 5c). This bias due to droplet interactions determines the division axes. In our numerical calculations, boundary conditions also influence the droplet divisions and slightly modify the division axes (see Fig. 5a).

Could such droplet division occur in experiments and what conditions are needed? To address this question, we provide in Table 1 two examples of parameter sets for which droplets would divide. These parameters are chosen such that dividing droplets would have a diameter of several micrometres and the material in the droplet would turn over in about two minutes. In case I, the surface tension is chosen small, similar to surface tensions that can be found in colloidal droplets or protein liquid phases[3]. The interfacial width in this case is of the order of ten nanometres. Case II describes droplets with a surface tension similar to that of oil/water interfaces with an interface thickness of about one nanometre. These examples show that small droplets that could be observable under the microscope could indeed undergo droplet division for plausible rates of chemical reactions and realistic interfacial tensions. However, as shown in Supplementary Information IV, droplet division for macroscopic droplets of millimetre or centimetre size will be difficult to achieve.

Chemically active droplets as a model for protocells

In this paper we have introduced a simple model to show that chemically active droplets can undergo cycles of growth and division reminiscent of cells. Our model combines the set of features that are minimally required for droplet division: two different chemical components undergoing reactions; phase separation; external energy input that maintains the system away from thermodynamic equilibrium. Our work shows that such droplet division would be expected to occur in small droplets. It will be an important challenge to observe this droplet division in future experiments. We have provided in Table 1 examples of parameter values for which micrometre-sized droplets would divide. These parameter values could in principle be achieved in artificial droplets or in *in vitro* studies of protein droplets.

The fact that active droplets tend to become unstable and divide is an unusual behaviour of droplets because surface tension usually opposes such shape changes. An instability of the droplet shape requires non-equilibrium conditions. In our model, these non-equilibrium conditions are provided by the energy input of a chemical fuel. The resulting chemical reactions drive diffusive fluxes across characteristic length scales as known for reaction–diffusion systems[22,23]. In the presence of droplet interfaces, these fluxes can induce a shape instability of stationary droplets. In the absence of chemical reactions and the resulting fluxes, the shape instability does not occur. The shape instability leading to droplet division introduced here can be compared to the Mullins–Sekerka instability often discussed in the context of crystal growth[24] (also see Supplementary Information). Both instabilities require a diffusion flux toward the interface. In the case of the Mullins–Sekerka instability the shape of a growing aggregate becomes unstable. For example, an interface can become unstable with respect to growing spikes called dendrites beyond a critical interface velocity. In contrast, the chemical-reaction-induced shape instability discussed here can occur for a stationary, non-growing droplet. This difference is important because in the case of a Mullins–Sekerka instability, the instability of a droplet does not lead to a shrinking waistline and fission but rather to the formation of a growing dendritic structure[25]. Only for the instability of a steady-state droplet found here does the instability generate a narrowing of the waistline of the initial droplet shape leading to fission in two droplets (see Supplementary Information III).

We propose that active droplets that turn over by chemical reactions provide a simple model for prebiotic protocells. The nature of such protocells remains unknown. While evolution can be reconstructed to a large extent both from fossil records and from the phylogenetic analysis of today's genomes, the structure and nature of early life forms remain quite unclear[26]. This leads to many interesting questions. How did the first replicating cells emerge from prebiotic precursors? Since replication involves specific chemical reactions, early replicators had to spatially organize chemistry and to concentrate certain molecules to facilitate reactions that would be unlikely in dilute or disorganized situations. Therefore, protocells as containers for chemical reactions had to appear.

Alexander Oparin pioneered the idea that macromolecular aggregation could lead to the formation of 'coacervates', liquid droplets that could organize chemistry and provide microreactors in which selected molecules were concentrated for prebiotic chemistry[1,27]. What types of molecules could have formed such droplets? It is interesting to note that modern-day cells possess a number of chemical compartments that are not separated by a membrane from the cell cytoplasm but that form by phase separation from the cytoplasm[3,7,28,29]. Many of these compartments are liquid and consist of RNA molecules and RNA-binding proteins[30–33]. The RNA world hypothesis suggests that at the origin of life, RNA was both the carrier of genetic information and could have acted as early enzymes[34,35]. Folded RNA molecules called ribozymes can be catalysts for many reactions including RNA processing[36]. Combining RNA with other molecules such as simple peptides may have been sufficient to organize RNA in liquid droplets[4]. The steps from chemically active droplets to the first dividing cells with membranes pose a big challenge to the understanding of early evolution. While it has been suggested that ribozymes that replicate RNA could have formed by molecular evolution[35,37], it is unclear how a cell membrane and cell division could have emerged[38–41].

The possibility that droplets may spontaneously divide has been discussed in the context of either negative surface tension[42,43] or in active nematic droplets[44]. Here we show that simply adding a proto-metabolism to droplets formed by classical phase separation can naturally lead to droplet division despite their surface tension. Membranes or surfactants are therefore not required to achieve

Table 1 | Examples of parameter values for dividing droplets.

	$D_{\pm}$ ($\mu m^2\,s^{-1}$)	w (nm)	γ (mN m^{-1})	$c_-^{(0)}$ (mM)	$c_+^{(0)}$ (mM)	ν_- (mM s^{-1})	$l_{\pm}$ (mm)	ϵ	t_R (s)	R_{div} (μm)
Case I	10	10	10^{-3}	100	1	1	0.1	2×10^{-3}	100	3
Case II	10	1	10	10^3	10^{-3}	10	5	8×10^{-4}	100	1

Parameters are defined in the Methods. For these parameters, the resulting supersaturation ϵ, the turnover time $t_R = c_-^{(0)}/\nu_-$, and the radius R_{div} where the stationary droplet shape becomes unstable are given. Case I is motivated by colloidal droplets or liquid protein phases with low surface tension. For Case II we chose properties of typical water/oil droplets.

division of prebiotic cells. Active droplets are natural systems to organize the chemistry of replicators and to form protocells. Such droplets can in principle form spontaneously by a rare nucleation event. Once they exist, they grow and divide. They provide a container for chemical reactions and they concentrate selected molecules that have an affinity to the droplet phase. The liquid and dynamic nature of active droplets implies that components in the droplet can mix and chemical reactions are facilitated. Protocells formed by active droplets require a constant energy supply, which could have been provided by a chemical fuel, by tides, or by temperature gradients, for example, in hydrothermal vents on the seafloor[2,45–47]. The chemical reactions by which new droplet material is formed and subsequently degraded represent an early metabolism. It will be interesting to generalize our study to systems with many droplets of different type. This corresponds to prebiotic ecosystems in which droplets may have 'symbiotic' relationships if one produces the nutrient of the other. Alternatively one may find predator–prey relationships when a droplet fuses with a different one to harvest its resources.

The possibility that early protocells were active membraneless droplets suggests possible scenarios by which cell membranes could have appeared. The droplet surface is an interface that will in general attract certain types of amphiphilic molecule. Such molecules have an affinity neither for the droplet phase nor for the surrounding fluid. As a result, selected molecules might populate the droplet surface and surface chemical reactions could be established. If lipids were available in the outside fluid, lipid monolayers or bilayers could be attracted to the specific droplet surface chemistry. Our work shows that active droplets can naturally divide. Therefore, protocells could have obtained their membranes long after the first dividing cells had appeared on Earth.

Methods

Methods, including statements of data availability and any associated accession codes and references, are available in the [online version of this paper](#).

References

1. Oparin, A. I. *Origin of Life* (Dover, 1952).
2. Haldane, J. B. S. The origin of life. *Ration. Annu.* **148,** 3–10 (1929).
3. Brangwynne, C. P. *et al.* Germline P granules are liquid droplets that localize by controlled dissolution/condensation. *Science* **324,** 1729–1732 (2009).
4. Koga, S., Williams, D. S., Perriman, A. W. & Mann, S. Peptide-nucleotide microdroplets as a step towards a membrane-free protocell model. *Nat. Chem.* **3,** 720–724 (2011).
5. Crosby, J. *et al.* Stabilization and enhanced reactivity of actinorhodin polyketide synthase minimal complex in polymer–nucleotide coacervate droplets. *Chem. Commun.* **48,** 11832 (2012).
6. Sokolova, E. *et al.* Enhanced transcription rates in membrane-free protocells formed by coacervation of cell lysate. *Proc. Natl Acad. Sci. USA* **110,** 11692–11697 (2013).
7. Hyman, A. A., Weber, C. A. & Jülicher, F. Liquid-liquid phase separation in biology. *Annu. Rev. Cell Dev. Biol.* **30,** 39–58 (2014).
8. Tang, T.-Y. D., van Swaay, D., DeMello, A., Ross Anderson, J. L. & Mann, S. *In vitro* gene expression within membrane-free coacervate protocells. *Chem. Commun.* **51,** 11429–11432 (2015).
9. Bray, A. Theory of phase-ordering kinetics. *Adv. Phys.* **43,** 357–459 (1994).
10. Ostwald, W. Studien über die Bildung und Umwandlung fester Körper. *Z. Phys. Chem.* **22,** 289–330 (1897).
11. Lifshitz, I. M. & Slyozov, V. V. The kinetics of precipitation from supersaturated solid solutions. *J. Phys. Chem. Solids* **19,** 35–50 (1961).
12. Binder, K. & Stauffer, D. Statistical theory of nucleation, condensation and coagulation. *Adv. Phys.* **25,** 343–396 (1976).
13. Voorhees, P. W. Ostwald ripening of two-phase mixtures. *Annu. Rev. Mater. Sci.* **22,** 197–215 (1992).
14. Zwicker, D., Decker, M., Jaensch, S., Hyman, A. A. & Jülicher, F. Centrosomes are autocatalytic droplets of pericentriolar material organized by centrioles. *Proc. Natl Acad. Sci. USA* **111,** E2636–E2645 (2014).
15. Zwicker, D., Hyman, A. A. & Jülicher, F. Suppression of Ostwald ripening in active emulsions. *Phys. Rev. E* **92,** 012317 (2015).
16. Puri, S. & Frisch, H. Segregation dynamics of binary mixtures with simple chemical reactions. *J. Phys. A* **27,** 6027–6038 (1994).
17. Glotzer, S. C., Stauffer, D. & Jan, N. Monte Carlo simulations of phase separation in chemically reactive binary mixtures. *Phys. Rev. Lett.* **72,** 4109–4112 (1994).
18. Carati, D. & Lefever, R. Chemical freezing of phase separation in immiscible binary mixtures. *Phys. Rev. E* **56,** 3127–3136 (1997).
19. Huggins, M. L. Solutions of long chain compounds. *J. Chem. Phys.* **9,** 440 (1941).
20. Flory, P. I. Thermodynamics of high polymer solutions. *J. Chem. Phys.* **10,** 51–61 (1942).
21. Oparin, A. *Proiskhozhedenie Zhizni Mosckovskii Rabochii* (Reprinted and translated in JD Bernal (1967) The Origin of Life London; Weidenfeld and Nicolson, 1924).
22. Turing, A. The chemical basis of morphogenesis. *Phil. Trans. R. Soc. Lond.* **237,** 37–72 (1952).
23. Gierer, A. & Meinhardt, H. A theory of biological pattern formation. *Biol. Cybern.* **12,** 30–39 (1972).
24. Mullins, W. W. & Sekerka, R. F. Morphological stability of a particle growing by diffusion or heat flow. *J. Appl. Phys.* **34,** 323–329 (1963).
25. Langer, J. S. Instabilities and pattern formation in crystal growth. *Rev. Mod. Phys.* **52,** 1–28 (1980).
26. Woese, C. R., Kandler, O. & Wheelis, M. L. Towards a natural system of organisms: proposal for the domains Archaea, Bacteria, and Eucarya. *Proc. Natl Acad. Sci. USA* **87,** 4576–4579 (1990).
27. Fox, S. W. The evolutionary significance of phase-separated microsystems. *Orig. Life* **7,** 49–68 (1976).
28. Brangwynne, C. P. Soft active aggregates: mechanics, dynamics and self-assembly of liquid-like intracellular protein bodies. *Soft Matter* **7,** 3052–3059 (2011).
29. Toretsky, J. A. & Wright, P. E. Assemblages: functional units formed by cellular phase separation. *J. Cell Biol.* **206,** 579–588 (2014).
30. Weber, S. C. & Brangwynne, C. P. Getting RNA and protein in phase. *Cell* **149,** 1188–1191 (2012).
31. Elbaum-Garfinkle, S. *et al.* The disordered P granule protein LAF-1 drives phase separation into droplets with tunable viscosity and dynamics. *Proc. Natl Acad. Sci. USA* **112,** 7189–7194 (2015).
32. Molliex, A. *et al.* Phase separation by low complexity domains promotes stress granule assembly and drives pathological fibrillization article phase separation by low complexity domains promotes stress granule assembly and drives pathological fibrillization. *Cell* **163,** 123–133 (2015).
33. Lin, Y. *et al.* Formation and maturation of phase-separated liquid droplets by RNA-binding proteins article formation and maturation of phase-separated liquid droplets by RNA-binding proteins. *Mol. Cell* **60,** 1–12 (2015).
34. Gilbert, W. Origin of life: the RNA world. *Nature* **319,** 618 (1986).
35. Higgs, P. G. & Lehman, N. The RNA World: molecular cooperation at the origins of life. *Nat. Rev. Genet.* **16,** 7–17 (2015).
36. Fedor, M. J. & Williamson, J. R. The catalytic diversity of RNAs. *Nat. Rev. Mol. Cell Biol.* **6,** 399–412 (2005).
37. Unrau, P. J. & Bartel, D. P. RNA-catalysed nucleotide synthesis. *Nature* **395,** 260–263 (1998).

38. Hanczyc, M. M., Fujikawa, S. M. & Szostak, J. W. Experimental models of primitive cellular compartments: encapsulation, growth, and division. *Science* **302,** 618–622 (2003).

39. Hanczyc, M. M. & Szostak, J. W. Replicating vesicles as models of primitive cell growth and division. *Curr. Opin. Chem. Biol.* **8,** 660–664 (2004).

40. Macía, J. & Solé, R. V. Synthetic Turing protocells: vesicle self-reproduction through symmetry-breaking instabilities. *Phil. Trans. R. Soc. B* **362,** 1821–1829 (2007).

41. Murtas, G. Early self-reproduction, the emergence of division mechanisms in protocells. *Mol. Biosyst.* **9,** 195–204 (2013).

42. Browne, K. P., Walker, D. A., Bishop, K. J. M. & Grzybowski, B. A. Self-division of macroscopic droplets: partitioning of nanosized cargo into nanoscale micelles. *Angew. Chem. Int. Ed. Engl.* **49,** 6756–6759 (2010).

43. Patashinski, A. Z., Orlik, R., Paclawski, K., Ratner, M. A. & Grzybowski, B. A. The unstable and expanding interface between reacting liquids: theoretical interpretation of negative surface tension. *Soft Matter* **8,** 1601–1608 (2012).

44. Giomi, L. & DeSimone, A. Spontaneous division and motility in active nematic droplets. *Phys. Rev. Lett.* **112,** 147802 (2014).

45. Baross, J. & Hoffman, S. Submarine hydrothermal vents and associated gradient environments as sites for the origin and evolution of life. *Orig. Life Evol. Biosph.* **15,** 327–345 (1985).

46. Martin, W. F. Hydrogen, metals, bifurcating electrons, and proton gradients: the early evolution of biological energy conservation. *FEBS Lett.* **586,** 485–493 (2012).

47. Martin, W. F., Sousa, F. L. & Lane, N. Evolution. Energy at life's origin. *Science* **344,** 1092–1093 (2014).

Additional information

Supplementary information is available in the online version of the paper. Reprints and permissions information is available online at www.nature.com/reprints. Correspondence and requests for materials should be addressed to F.J.

Competing financial interests

The authors declare no competing financial interests.

Methods

Reaction rates and energy supply. The chemical reaction $A \rightleftharpoons B$ converts soluble precursors A to droplet material B with forward reaction flux $s_\rightarrow$ and reverse flux $s_\leftarrow$. The net reaction flux $s = s_\rightarrow - s_\leftarrow$ characterizes the concentration per unit time that is undergoing the reaction. Compatibility with thermodynamics requires[48]

$$\frac{s_\rightarrow}{s_\leftarrow} = \exp\left(-\frac{\Delta\mu}{k_B T}\right) \qquad (3)$$

where $\Delta\mu$ is the chemical free energy change associated with the forward reaction. This condition leads to detailed balance of forward and backward reaction rates at chemical equilibrium. The net reaction flux s can therefore be written as

$$s = s_\leftarrow \left[\exp\left(-\frac{\Delta\mu}{k_B T}\right) - 1\right] \qquad (4)$$

Chemical equilibrium is reached when $\Delta\mu = 0$ and the net reaction flux vanishes, $s = 0$. If as in (1) the reaction does not involve other reaction partners or external energy input, the chemical free energy change $\Delta\mu = \Delta\mu^{(1)}$ is given by the difference of the chemical potentials,

$$\Delta\mu^{(1)} = \mu_B - \mu_A \qquad (5)$$

Such a reaction leads to spontaneous degradation of B and formation of A if $\mu_B > \mu_A$ and thus $\Delta\mu^{(1)} > 0$. The chemical potentials of a molecular species n can be written as $\mu_n = k_B T \ln(v_n c_n) + w_n$, where v_n is a molecular volume and c_n the concentration of species n. The first term is of entropic origin while the contribution w_n is mainly enthalpic and includes internal molecular free energies and interaction energies between molecules. Note that w_n generally depends on composition, and thus has different values inside and outside the droplet.

The net reaction rate corresponding to reaction pathway (1) can thus be written as

$$s^{(1)} = s_\leftarrow^{(1)}\left(\frac{c_A}{c_B} K^{(1)} - 1\right) \qquad (6)$$

where $K^{(1)} = (v_A/v_B)\exp((w_A - w_B)/k_B T)$ is the equilibrium constant of reaction pathway (1). Note that in the case of phase separation, $K^{(1)}$ and $s_\leftarrow^{(1)}$ can have different values inside and outside the droplet. If only reaction pathway (1) occurs, droplets are passive despite the presence of the reaction and the system reaches a thermodynamic equilibrium. No droplet divisions occur. Such a system exhibits Ostwald ripening and after long times reaches an equilibrium that contains either a single large droplet or no droplet.

Active droplets require an external energy supply that maintains the droplets away from thermodynamic equilibrium at all times. The reaction $A \rightleftharpoons B$ can be coupled to an externally supplied fuel C with reaction product C' with chemical potential difference $\Delta\mu_C = \mu_C - \mu_{C'} > 0$. This second reaction pathway (2) obeys equation (4) with $\Delta\mu = \Delta\mu^{(2)}$ and

$$\Delta\mu^{(2)} = \mu_B - \mu_A - \Delta\mu_C \qquad (7)$$

The corresponding reaction flux can be written as

$$s^{(2)} = s_\leftarrow^{(2)}\left(\frac{c_A}{c_B} K^{(2)} - 1\right) \qquad (8)$$

with equilibrium constant $K^{(2)} = K^{(1)}\exp(\Delta\mu_C/k_B T)$. If both pathways are active at the same time, the net reaction flux is $s = s^{(1)} + s^{(2)}$. In this paper we consider the case where an active droplet converts B to A inside the droplet mainly via the reaction pathway (1) while outside the droplet material A is used to generate B mainly via the reaction pathway (2) using the external fuel as an energy source (see Fig. 2 and Supplementary Information). No chemical equilibrium can be reached in this case because the equilibrium constants $K^{(1)}$ and $K^{(2)}$ imply incompatible equilibrium conditions. The droplet is thus active.

Dynamics of active droplets. We consider a fluid that contains the droplet-forming material B at concentration $c = c_B$. The system segregates into two coexisting phases that are separated by a sharp interface. We consider the limit of strong segregation of phases by a sharp interface. Across the interface, chemical potentials are continuous, $\mu_+ = \mu_-$, while the pressure exhibits a jump

$$P_- - P_+ = 2\gamma H \qquad (9)$$

known as Laplace pressure. Here, γ denotes surface tension and H denotes the local mean curvature of the interface. The subscripts $-$ and $+$ refer to values at the interface inside and outside the droplet, respectively. These thermodynamic conditions determine the concentrations c_- and c_+ at the interface where both phases coexist. As the Laplace pressure depends on local curvature, the equilibrium concentrations also depend on curvature H. We express this dependence to linear order by

$$c_\pm \simeq c_\pm^{(0)} + \gamma\beta_\pm H \qquad (10)$$

where $c_\pm^{(0)}$ denote the equilibrium concentrations of coexisting phases at a flat interface and we have introduced the coefficients $\beta_\pm$ to describe the effects of interface curvature.

The droplet material B is produced by chemical reactions with total reaction flux s, which is a function of concentration (see Fig. 3a and the section 'Reaction rates and energy supply'). The time evolution of the concentration field c is then described by the reaction–diffusion equation

$$\partial_t c = D_\pm \nabla^2 c + s \qquad (11)$$

where D_+ and D_- denote the diffusion coefficients outside and inside the droplet, respectively. The evolution of the droplet shape is governed by the normal velocity of the droplet interface

$$v_n = \frac{j_- - j_+}{c_- - c_+} \qquad (12)$$

where $j_\pm = -\mathbf{n} \cdot D_\pm \nabla c$ are the normal diffusion fluxes at the interface, inside and outside the droplet, and $\mathbf{n}$ denotes the surface normal.

The reaction flux is typically positive (B is produced) outside the droplet, while it is negative (A is produced) inside (see Fig. 3a). We expand the function $s(c)$ introduced in the section 'Reaction rates and energy supply' in terms of the concentration variations inside and outside the droplet to linear order as (see Supplementary Information)

$$s(c) \simeq \begin{cases} v_+ - k_+(c - c_+^{(0)}) & \text{outside the droplet} \\ -v_- - k_-(c - c_-^{(0)}) & \text{inside} \end{cases} \qquad (13)$$

The reaction rates $k_\pm$ inside and outside the droplet are related to elasticity coefficients of the chemical reactions[49]. The fluxes of production of B molecules at the equilibrium concentrations outside and inside the droplet are denoted v_+ and v_-, respectively. We call v_- turnover because it is the flux at which B molecules disappear inside the droplet. The concentration field varies over the characteristic length scales $l_\pm = (D_\pm/k_\pm)^{1/2}$ inside and outside the droplet, respectively.

At large distances $r \gg l_+$ from the droplet, the net reaction flux $s(c)$ vanishes and the concentration reaches the constant value $c_\infty = c_+^{(0)} + v_+/k_+$. The chemical reactions thus generate a supersaturation

$$\epsilon = \frac{c_\infty - c_+^{(0)}}{\Delta c} \qquad (14)$$

where $\Delta c = c_-^{(0)} - c_+^{(0)}$. This supersaturation drives the diffusion flux j_+ toward the droplet interface. Inside the droplet, droplet material is degraded, leading to a concentration profile with minimal concentration in the droplet centre. This causes a diffusion flux j_- towards the centre (see Fig. 3b).

Data availability. The data that support the plots within this paper and other findings of this study are available from the corresponding author on request.

References

48. Atkins, P. & de Paula, J. *Atkins' Physical Chemistry* (OUP Oxford, 2010).
49. Kacser, H., Burns, J. A. & Fell, D. A. The control of flux. *Biochem. Soc. Trans.* **23,** 341–366 (1995).